Enhanced temperature-dependent magnetoresistivity of Fe/Cr superlattices

Shufeng Zhang* and Peter M. Levy
Department of Physics, New York University, 4 Washington Place, New York, New York 10003
(Received 13 November 1990)

The temperature dependence of the magnetoresistivity is found to be much larger in Fe/Cr superlattices with rough interfaces (high magnetoresistance) than those with sharp ones (small magnetoresistance). We discuss the mechanisms which produce this temperature dependence and point out that symmetry conditions restrict the putative mechanisms in superlattices. We show that the enhanced temperature dependence of the magnetoresistance can be explained by the existence of local spin excitations at the roughened Fe/Cr interfaces.

I. INTRODUCTION

The resistivities of several iron-chromium (Fe/Cr) superlattices were measured as a function of temperature between 4.2 and 300 K in the ferromagnetic ($H > H_{\rm sat}$) and antiferromagnetic ($H=0$) configurations.[1] The salient observation was that superlattices with low resistivity (sharper interfaces) have very small magnetoresistance *and* weak temperature dependence of the resistivity; superlattices with larger magnetoresistance (rougher interfaces) have a large temperature dependence of their resistivity and magnetoresistance. The ineluctable conclusion to be drawn is that the *enhanced* temperature dependence of the resistivity comes from the increased interface roughness scattering due to rougher interfaces. While this increased resistivity due to interface scattering has been recognized at $T=0$ K,[2] its role in enhancing the temperature dependence of the resistivity and magnetoresistance has only now been established by Petroff *et al.*[1]

Here we discuss the possible mechanisms that produce temperature dependence of the resistivity of magnetic superlattices, and we indicate which one is the probable cause for the enhanced temperature dependence. We conclude that the dominant mechanism responsible for the temperature-dependent resistivity of ferromagnetic transition-metal-based alloys[3] is *not* responsible for the enhancement observed in Fe/Cr superlattices. Rather we show that the enhanced temperature dependence of the magnetoresistance can be explained by the existence of local spin excitations at the roughened Fe/Cr superlattices. By using a simplified model of spin-dependent interface scattering, we calculate the temperature dependence of the resistivity and compare our results to existing data on Fe/Cr superlattices.

II. TWO-CURRENT MODEL

The temperature dependence of the resistivity of ferromagnets has traditionally been analyzed in terms of the two-current model developed by Fert.[4] In the temperature range where the residual resistivities $\rho_{0\sigma}$ are much larger than $\rho_{i\sigma}(T)$ [$\equiv\rho_\sigma(T)-\rho_{0\sigma}$] and the spin-flip term $\rho_{\uparrow\downarrow}(T)$, the resistivity is given as[3]

$$\rho(T)=\rho_0+\left[1+\frac{(\alpha-\mu)^2}{(1+\alpha)^2\mu}\right]\rho_i(T)+\frac{(\alpha-1)^2}{(\alpha+1)^2}\rho_{\uparrow\downarrow}(T)\ , \tag{1}$$

where

$$\rho_0^{-1}=\sum_\sigma \rho_{0\sigma}^{-1}\ ,$$

$$\rho_i^{-1}(T)=\sum_\sigma \rho_{i\sigma}^{-1}(T)\ ,$$

$$\alpha\equiv\rho_{0\uparrow}/\rho_{0\downarrow}\ ,$$

and

$$\mu\equiv\rho_{i\uparrow}(T)/\rho_{i\downarrow}(T)\ .$$

While both phonons and magnons contribute to the temperature-dependent resistivities $\rho_{i\sigma}(T)$, only magnons give rise to spin-flip scattering and contribute to the spin-mixing term $\rho_{\uparrow\downarrow}(T)$.[5] From extensive comparisons of Eq. (1) to resistivity data of nickel-, iron,- and cobalt-based alloys,[3,6] it was found that the spin-mixing term is crucial in explaining the temperature dependence of the resistivity.

For those Fe/Cr superlattices which have sharper interfaces, as evidenced by lower resistivities and smaller magnetoresistances, Petroff *et al.*[1] found that the resistivity is weakly dependent on temperature. In fact, the temperature dependence is comparable to that found in bulk ferromagnetic iron alloys.[3] However, for those superlattices with large magnetoresistance, the temperature dependence of the resistivity is *enhanced.* The larger magnetoresistance and resistivity are associated with rougher interfaces between iron and chromium layers. We surmise that the increased roughness scattering at interfaces is responsible for the enhanced temperature dependence of the resistivity. This can come from increasing the spin-conserving contribution proportional to $\rho_i(T)$ *or* the spin-mixing term $\rho_{\uparrow\downarrow}(T)$.

The spin-conserving term comes from self-energy corrections to the conduction-electron propagators that are temperature dependent, e.g., phonons, magnons, and electron-electron scattering, as well as vertex corrections

 ©1991 The American Physical Society

that do *not* involve spin flips. However, the spin-mixing term comes from *vertex corrections* to the conductivity, which comes from spin-flip scattering events in which momentum is transferred from one spin channel to the other, but in which dissipation is not necessarily involved. This term is proportional to[7]

$$\rho_{\uparrow\downarrow}(T)\sim\int d^3k\int d^3k'(\mathbf{k}\cdot\hat{\mathbf{u}})(\mathbf{k}'\cdot\hat{\mathbf{u}})J^2(\mathbf{k}\uparrow,\mathbf{k}'\downarrow)n_{\mathbf{q}}(T)\times\delta(\varepsilon_{k\uparrow}-\varepsilon_{k'\downarrow}+h\omega_{\mathbf{q}})\ , \quad (2)$$

where $\mathbf{q}\equiv\mathbf{k}'-\mathbf{k}$, $\hat{\mathbf{u}}$ is a unit vector in the direction of the electric field, $J(\mathbf{k}\sigma,\mathbf{k}'\sigma')$ is the matrix element of the spin flip scattering, and $\omega_{\mathbf{q}}$ and $n_{\mathbf{q}}$ are the frequency and occupancy of the magnons.

The spin-mixing term [Eq. (2)] has been evaluated for scattering in bulk materials in which *extended* excitation (magnons) with *well-defined energy-momentum* relations exist.[4,7] This term exists in Fe/Cr superlattices to the extent that scattering by the iron layers is from extended magnon modes $\omega(\mathbf{q})$, and it inevitably contributes to the temperature dependence of the resistivity observed in superlattices with small magnetoresistances (and therefore sharp interfaces). However, we believe this cannot account for the enhanced temperature dependence of the resistivity seen in superlattices with rough interfaces. In Fig. 1 we show the temperature-dependent resistivity of the superlattices with large magnetoresistance after removing the small temperature-dependent part of the resistivity of superlattices with small magnetoresistance. In the terminology of Petroff *et al.*,[1] this is the sum of the residual resistivity and $\Delta\rho(T)$ [see Fig. 3(a) of Ref. 1]. This difference in the temperature-dependent resistivities indubitably arises from the *same* mechanism that produces the large magnetoresistance. We note that the differences $\Delta\rho(T)$ for $H=0$ and $H>H_S$ are nearly *independent* of temperature for $T<50$ K. We conclude that the energy of the modes that give rise to this temperature-dependent scattering cannot extend down to zero. Rather the excitation spectrum which give rise to the temperature-dependent resistivity *above that found in samples with small magnetoresistances* probably has a gap near $\omega=0$ and has higher-energy modes which *start* to be populated only for $T>50$ K. In contrast, superlattices with small magnetoresistance have a temperature-dependent resistivity which is reminiscent of that coming from extended excitations which have a energy spectrum going down to $\omega=0$.

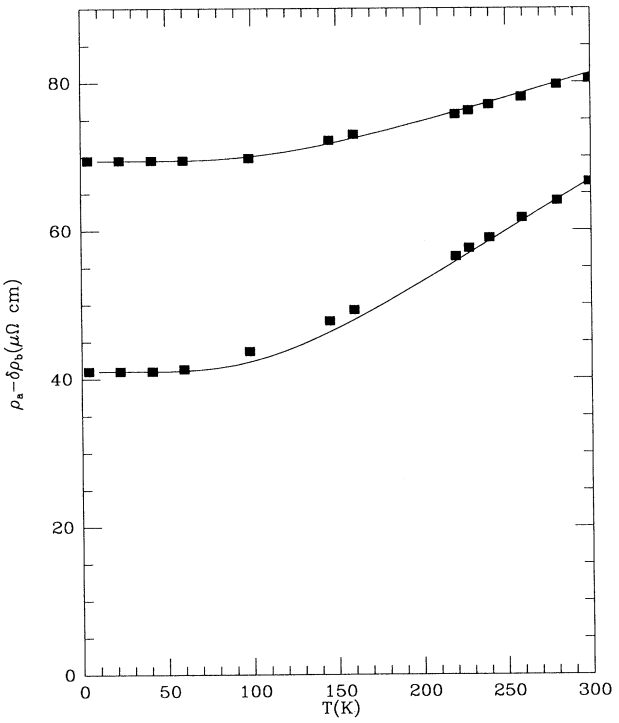

FIG. 1. Square points are the resistivity for $H=0$ (upper curve) and $H>H_S$ (lower curve) for [Fe(16 Å)/Cr(12 Å)]$_{18}$ (see Ref. 1), *after the temperature-dependent resistivity of the "background"* [taken to be the temperature-dependent resistivity shown in Fig. 3(b) of Ref. 1] *has been subtracted.* Aside from the residual resistivities at $T=0$ K, these curves correspond to the quantity $\Delta\rho(T)$ ($H=0$) and $\Delta\rho_H(T)$ ($H>H_S$) shown in Fig. 3(a) of Ref. 1. The solid lines are our calculated fits.

From the above observations we conclude—and, in the next section, we justify by an explicit calculation—that the scattering of conduction electrons at rough interfaces comes from localized magnon (impurity) modes which do not have well-defined $\omega(\mathbf{q})$ relations. When a conduction electron scatters off a *localized* magnon, momentum is not conserved. In this case, the spin-mixing term Eq. (2) is proportional to

$$\rho_{\uparrow\downarrow}(T)\sim\int d\hat{\mathbf{k}}\int d\hat{\mathbf{k}}'(\hat{\mathbf{k}}\cdot\hat{\mathbf{u}})(\hat{\mathbf{k}}'\cdot\hat{\mathbf{u}})J(\mathbf{k}\uparrow,\mathbf{k}'\downarrow)^2\ , \quad (3)$$

where the carets denote unit vectors; i.e., we are averaging over solid angles $\Omega_{\hat{\mathbf{k}}}$ and $\Omega_{\hat{\mathbf{k}}'}$. It should be noted that the magnon momentum does not enter Eq. (3) as it is not conserved. We expand the momentum dependence of the scattering in terms of spherical waves of angular momentum l,

$$J(\mathbf{k},\mathbf{k}')\approx\sum_l J_l(k,k')Y_l(\hat{\mathbf{k}})Y_l(\hat{\mathbf{k}}')\ . \quad (4)$$

For local modes to contribute to spin mixing, it is necessary that scattering occurs in angular momentum channels with *opposite parities.*[8] *In Fe/Cr* superlattices, the dominant spin-dependent scattering of conduction electrons comes from the *s-d*-mixing interaction;[9] therefore, it acts primary in the $l=2$ channel of the conduction electrons. Coulomb scattering occurs in all channels; in particular, $l=1$ and 3, but for it to be effective the conduction electrons being scattered at the Fe/Cr interface must have an $l=1$ or 3 partial density of states near the Fermi surface. Therefore, we find contributions to the spin-mixing term $\rho_{\uparrow\downarrow}(T)$ from the temperature-dependent spin-flip scattering of localized excitations (as distinct from extended modes) is limited to situations where the density of states of conduction electrons near the Fermi surface has angular momentum components with opposite parities.

The spin-conserving temperature-dependent resistivity term from localized excitations, which is proportional to

$$\rho_\sigma(T)\sim \int d\hat{\mathbf{k}} \int d\hat{\mathbf{k}}'\, k^2 J(\mathbf{k},\mathbf{k}')^2 , \tag{5}$$

does not have this restriction. Therefore, unless there is some proof that the conduction electrons near the Fermi surface in Fe/Cr superlattices have appreciable p-wave character (or f-wave character, which is less likely), one should ascribe the enhancement of the temperature dependence of the resistivity in Fe/Cr superlattices with rough interfaces to the spin-conserving term, e.g., the conduction-electron self-energy corrections, rather than the spin-mixing term, which is a vertex correction.

III. MODEL CALCULATION OF TEMPERATURE DEPENDENCE

To calculate the temperature-dependent resistivity coming from the *spin-conserving* terms for a magnetic *superlattice,* we rely on the formalism developed to explain, *inter alia,* the giant magnetoresistance of Fe/Cr superlattices.[2] As this has been formulated by using the Kubo formalism rather than the Boltzmann approach, we have derived in Appendix A the relationship between the two-current model of Fert and the spin-dependent resistivity based on the Kubo formalism.

We have argued in Sec. II that vertex corrections (spin flip) are not the primary cause for the enhanced temperature dependence of the magnetoresistance for superlattices with rough interfaces. The same parity arguments apply to vertex corrections which do not involve spin flips, i.e., due to phonons and the longitudinal part of the spin scattering, $jS_{lz}\sigma_z$. Vertex corrections (spin flip and spin conserving) do exist from scattering within the layers as these can come from extended modes. From the data of Petroff *et al.*[1] the temperature-dependent resistivity resulting from these excitations, as well as other sources, is quite small compared with that coming from roughened interfaces. For this reason and because we have not yet developed the formalism for calculating the vertex corrections for multilayered structures, we focus our attention on calculating the temperature-dependent magnetoresistivity arising from the localized interfacial modes that contribute to the conduction-electron self-energy term. To account for the entire temperature dependence of the resistivity seen in Fe/Cr superlattices with roughened interfaces, we will supplement our result with the small variation of resistivity with temperature observed in superlattices with sharp interfaces.

The enhanced temperature-dependent resistivity due to localized magnon scattering at interfaces (induced by their roughness) is calculated by considering only the simple bubble diagrams in the Kubo formalism (see Appendix A). The spin-dependent scattering at an Fe/Cr interface is modeled by the potential[2]

$$V_s(\mathbf{r},\hat{\boldsymbol{\sigma}})=\sum_l (v+j\hat{\boldsymbol{\sigma}}\cdot\mathbf{S}_l) f_l(\rho)\delta(z-z_l) , \tag{6}$$

where

$$\mathbf{S}_l=\frac{1}{M_0}\sum_{i\in l}\mathbf{S}_i .$$

Here z_l represents the position of the interface,

$$M_0\equiv\sum_{i\in l} S_i = S\sum_{i\in l} 1 ,$$

if all spins are equal in magnitude, $\mathbf{S}_i$ is the spin of an impurity atom at an interface, e.g., iron where chromium should be or vice versa, $\hat{\boldsymbol{\sigma}}$ is a Pauli matrix which represents the spin of a conduction electron, and $f_l(\rho)$ is a random function representing the surface roughness ($\rho=x,y$). As we will use the spin-wave approximation, we must refer the spin operator $\mathbf{S}_l$ to the axis $\hat{\mathbf{M}}_l$, which represents the direction of the iron magnetization adjacent to the lth interface. On the contrary the conduction-electron spin operator $\hat{\sigma}$ should be quantized along the direction of resultant magnetization of the superlattice, i.e., along the externally applied field when there is no anisotropy, so that the self-energy $\Delta^{\sigma\sigma'}$ is diagonal in spin space.[2]

Here we first consider the case that the magnetization axis $\hat{\mathbf{M}}_{\mathrm{Fe}}$ is parallel to the axis of quantization for $\hat{\boldsymbol{\sigma}}$; the extension to general angles is straightforward. Therefore, the scalar product $\hat{\boldsymbol{\sigma}}\cdot\mathbf{S}_l$ is written as

$$\hat{\boldsymbol{\sigma}}\cdot\mathbf{S}_l=\frac{1}{M_0}\sum_{i\in l}[\sigma_z S_i^z+\sigma^- S_i^+ +\sigma^+ S_i^-] . \tag{7}$$

By combining Eqs. (6) and (7) and replacing the local spin operators by Bose annihilation and creation operators[10] (this is correct only when a single excitation is present, i.e., at low temperatures; otherwise, it is an approximation), we find that the second quantized form of Eq. (6) is

$$V_s=\sum_{k,\nu,k',\nu'}\sum_l e^{-i\bar{\nu}z_l}e^{i(k'-k)\rho}f_l(\rho)\left[\left[\sum_\sigma (v+j\sigma S_{lz})c^\dagger_{\mathbf{k}'\sigma}c_{\mathbf{k}\sigma}\right]+\frac{j\sqrt{2S}}{M_0}\sum_{i\in l}(a_i c^\dagger_{\mathbf{k}'\downarrow}c_{\mathbf{k}\uparrow}+a_i^\dagger c^\dagger_{\mathbf{k}'\uparrow}c_{\mathbf{k}\downarrow})\right] , \tag{8}$$

where $\mathbf{k}=(k,\nu)$, $k=k_x,k_y$, $\bar{\nu}\equiv\nu-\nu'$, and we have represented the local spin operator as

$$S_i^+=\sqrt{2S}\,a_i ,$$
$$S_i^-=\sqrt{2S}\,a_i^\dagger$$

and

$$S_{lz}=\frac{1}{M_0}\sum_{i\in l}(S-a_i^\dagger a_i) , \tag{9}$$

where a_i ($a_i^\dagger$) is the annihilation (creation) operator of a local magnon at the interface. To calculate the self-energy or t matrix for the potential Eq. (8), we use the unperturbed Hamiltonian

$$H_0=\sum_{\mathbf{k},\sigma}\varepsilon_{\mathbf{k}}c_{\mathbf{k}\sigma}^\dagger c_{\mathbf{k}\sigma}+\sum_{i\in l}\omega_i a_i^\dagger a_i \ , \tag{10}$$

where ω_i is the energy for a local excitation at site i. Also, we note that the t matrix is diagonal in momentum space parallel to the layer plane ($k=k'$), because the multilayered structures we consider are homogeneous in the planes parallel to the layers.

As we see from Eq. (8), the first term involves non-spin-flip (NSF) scattering, while the second has spin-flip (SF) scattering. The t matrix due to NSF is obtained by second-order perturbation, which gives

$$\begin{aligned} t_{\bar{v}}^{\mathrm{NSF}}(\varepsilon_F,\sigma,T)&=\sum_l e^{-i\bar{v}z_l}\langle f_l^2\rangle\left\langle\sum_{\mathbf{k}'}\frac{(v+j\sigma S_{lz})^2}{\varepsilon_F-\varepsilon_{\mathbf{k}'}+i\delta}\right\rangle_{\mathrm{th}} \\ &=-i\pi\sum_l e^{-i\bar{v}z_l}\langle f_l^2\rangle\rho(\varepsilon_F)\langle(v+j\sigma S_{lz})^2\rangle_{\mathrm{th}} \ , \end{aligned} \tag{11}$$

where the angular brackets $\langle\ \rangle_{\mathrm{th}}$ denote a thermal average, and $\langle f_l^2\rangle$ represents the average over interface roughness in a plane at z_l; we have neglected the real part of the sum over $\mathbf{k}'$ because it does not contribute to the conductivity. The thermal average for S_{lz} is

$$\begin{aligned} \langle S_{lz}\rangle_{\mathrm{th}}&=\frac{1}{M_0}\sum_{i\in l}\langle(S-a_i^\dagger a_i)\rangle_{\mathrm{th}} \\ &=1-\frac{1}{M_0}\sum_{i\in l}\langle a_i^\dagger a_i\rangle_{\mathrm{th}} \end{aligned} \tag{12}$$

and

$$\langle a_i^\dagger a_i\rangle_{\mathrm{th}}=n^B(\omega_i)=(e^{\beta\omega_i}-1)^{-1} \ ,$$

where ω_i is the energy of a local magnon at site i. In the approximation that each local magnon has the same energy ω_0, i.e., $\omega_i=\omega_0$, Eq. (12) becomes

$$\langle S_{lz}\rangle=1-\frac{1}{S}n^B(\omega_0) \ . \tag{13}$$

By placing Eq. (13) into Eq. (11), we find the t matrix for the non-spin-flip scattering is

$$t_{\bar{v}}^{\mathrm{NSF}}(\sigma)=-i\pi\sum_l e^{-i\bar{v}z_l}\langle f_l^2\rangle\rho(\varepsilon_F)\left[v+j\sigma\left[1-\frac{n^B(\omega_0)}{S}\right]\right]^2 \ , \tag{14}$$

where in our local spin-wave approximation (SWA) we set $\langle S_{lz}^2\rangle\approx\langle S_{lz}\rangle^2$.

The t matrix for spin-flip scattering, i.e., second term in Eq. (8), may be obtained by performing a Matsubara summation over the internal degree of freedom.[11] If we consider the one-magnon correction to the t matrix for the conduction electron, we have, for example, for the spin-down t matrix,

$$t_{\bar{v}}^{\mathrm{SF}}(\varepsilon_F,\sigma=\downarrow,T)=\sum_l e^{-i\bar{v}z_l}\langle f_l^2\rangle(\sqrt{2S}j)^2\frac{1}{M_0}\sum_{i\in l}\sum_{\mathbf{k}}\frac{1}{\beta}\sum_{ip}G_{\mathbf{k}}(\sigma=\uparrow,\varepsilon_F+ip)D_i(ip) \ , \tag{15}$$

where G and D_i are the propagators for conduction electrons and magnons,

$$G_{\mathbf{k}}(\sigma=\uparrow,\omega)=\frac{1}{\omega-\varepsilon_{\mathbf{k}}+i\delta}$$

and

$$D_i(ip)=\frac{1}{ip-\omega_i+i\delta} \ .$$

By performing the sum over frequency, we find

$$\frac{1}{\beta}\sum_{ip}G_{\mathbf{k}}(\sigma=\uparrow,\varepsilon_F+ip)D_i(ip)=\frac{n^B(\omega_i)+n^F(\varepsilon_{\mathbf{k}})}{\varepsilon_F+\omega_i-\varepsilon_{\mathbf{k}}+i\delta} \ , \tag{16}$$

where $n^F(\varepsilon_{\mathbf{k}})$ is the Fermi function. By placing Eq. (16) into (15) and integrating over $\mathbf{k}$, we find that the imaginary part of the SF contribution is

$$t_{\bar{v}}^{\mathrm{SF}}(\varepsilon_F, \sigma=\downarrow, T)=-i\pi\sum_l e^{-i\bar{v}z_l}\langle f_l^2\rangle\rho(\varepsilon_F+\omega_0)\times 2j^2[n^B(\omega_0)+n^F(\omega_0)]\ , \tag{17}$$

where we have used $n(\omega_i)=n(\omega_0)$. In the same manner, we have calculated the conduction-electron spin-up t matrix and find

$$t_{\bar{v}}^{\mathrm{SF}}(\varepsilon_F, \sigma=\uparrow, T)=t_{\bar{v}}^{\mathrm{SF}}(\varepsilon_F, \sigma=\downarrow, T)\ , \tag{18}$$

where we assumed a flat density of state for the conduction electrons, i.e., $\rho(\varepsilon_F\pm\omega_0)\approx\rho(\varepsilon_F)$. In the Appendix B, we show how Eq. (18) is arrived at by another route. The total t matrix is then found by adding Eqs. (14) and (17),

$$t_{\bar{v}}(\sigma, T)=-i\pi\sum_l e^{-i\bar{v}z_l}\Delta_l^{\sigma}(T)\ , \tag{19}$$

where

$$\Delta_l^{\sigma}(T)=\rho(\varepsilon_F)\langle f_l^2\rangle\{v^2+j^2[1-n^B(\omega_0)/S]^2+2vj\sigma[1-n^B(\omega_0)/S]+2j^2[n^B(\omega_0)+n^F(\omega_0)]\}\ . \tag{20}$$

We have extended the calculation to arbitrary angles θ_l, i.e., not restricted to $\theta_l=0$. With the spin operator $\mathbf{S}_l$ referred to a local axis $\hat{\mathbf{M}}_l$ making an angle θ_l with respect to the external field and $\hat{\sigma}$ referred to the field, the scalar product [Eq. (7)] is written as

$$\begin{aligned}\hat{\sigma}\cdot\mathbf{S}_l=&S_l^z[\cos\theta_l\,\sigma_z-\tfrac{1}{2}\sin\theta_l\,(\sigma_+ +\sigma_-)]+\tfrac{1}{2}S_l^+[\sin\theta_l\,\sigma_z-\sin^2(\theta_l/2)\sigma_+ +\cos^2(\theta_l/2)\sigma_-]\\&+\tfrac{1}{2}S_l^-[\sin\theta_l\,\sigma_z+\cos^2(\theta_l/2)\sigma_+ -\sin^2(\theta_l/2)\sigma_-]\ .\end{aligned} \tag{21}$$

By repeating our calculation [Eqs. (8)–(18)], we find that for arbitrary θ_l, Eq. (20) is replaced by

$$\Delta_l^{\sigma}(T)=\rho(\varepsilon_F)\langle f_l^2\rangle\{v^2+j^2[1-n^B(\omega_0)/S]^2+2vj\sigma\cos\theta_l[1-n^B(\omega_0)/S]+2j^2[n^B(\omega_0)+n^F(\omega_0)]\}\ . \tag{22}$$

The calculation of the resistivity for the t matrix in Eq. (19) is *identical* to our previous one.[2] Because of the inhomogeneous nature of scattering in layered structures, we introduce a position-dependent conductivity $\sigma(z)$; this has been explicitly obtained for zero temperature, i.e., $n^B(\omega_0)=n^F(\omega_0)=0$ in Eqs. (20) and (22). For finite temperatures we replace $\Delta_l^{\sigma}(T=0)$ in Ref. 2 by $\Delta_l^{\sigma}(T)$ of Eq. (22). Aside from the parameters for the $T=0$ K resistivity, only *one* additional parameter ω_0, the local magnon energy, is required for finite, nonzero temperatures in our simplified model of the interfacial scattering. We now describe our results.

IV. DISCUSSION OF RESULTS

The parameters to describe the magnetoresistance of the present [Fe(16 Å)/Cr(12 Å)]$_{18}$ sample[1] at $T=0$ K are very similar to those we used to fit a previous series of Fe/Cr samples,[2] i.e., $p=j/v=0.55$ for the ratio of spin-dependent to spin-independent scattering, $\lambda_s=(1.1/2)(a+b)=15.4$ Å for the spin-independent mean free path due to interfacial scattering, and $\lambda_b=23$ Å for the spin-independent mean free path due to bulk scattering (within the layers). Only the latter value is different from our previous one; for the previous series of Fe/Cr superlattices, we used $\lambda_b=19$ Å. These values fix the resistivities of the present sample at $T=0$ K for both $H=0$ and $H>H_S$.

The only new parameter ω_0 is fixed so as to reproduce the observed resistivity *increase* at $T=300$ K for $H>H_S$ (see Fig. 1, lower curve), which represents the difference in temperature-dependent resistivities between the [Fe(16 Å)/Cr(12 Å)]$_{18}$ sample with large magnetoresistance and

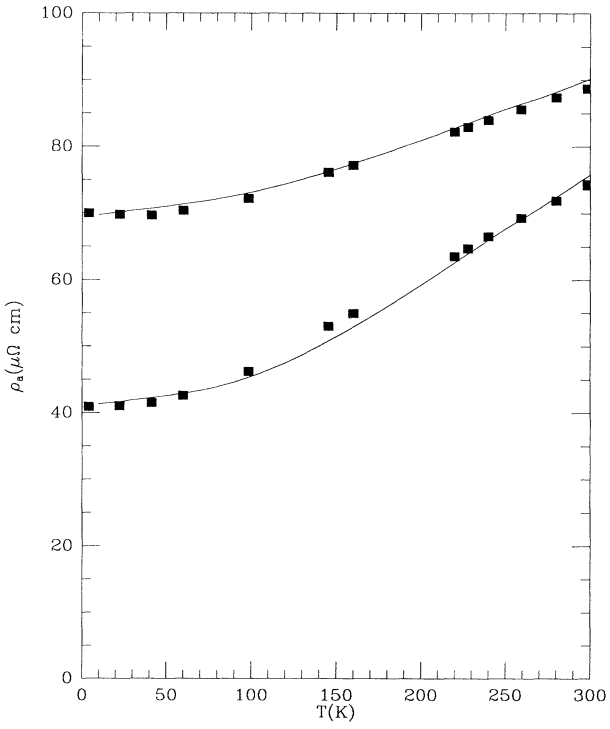

FIG. 2. Squares are the experimental data on the resistivity for $H=0$ (upper curve) and $H>H_S$ (lower curve) for [Fe(16 Å)/Cr(12 Å)]$_{18}$ taken from Ref. 1. The solid lines represent our calculated fits that have been *augmented* by the temperature-dependent resistivity of the "background," i.e., the temperature-dependent resistivity for a superlattice with small magnetoresistance (sharp interfaces) [see Fig. 3(b) of Ref. 1].

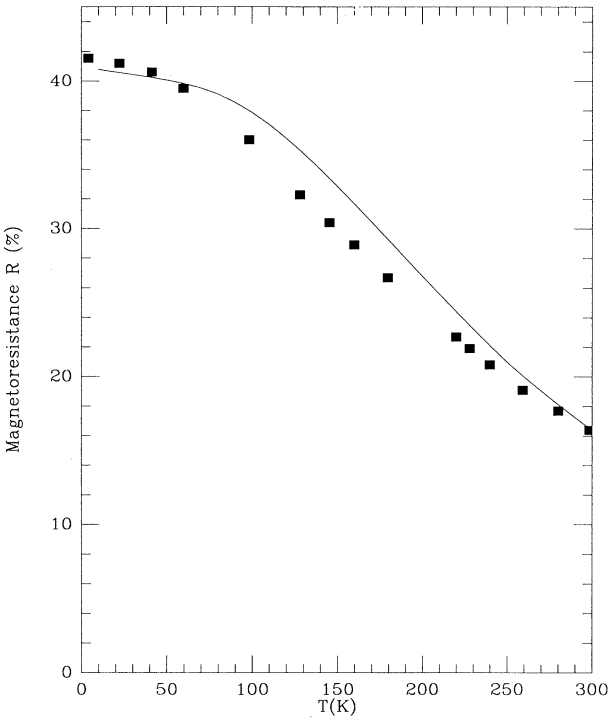

FIG. 3. Temperature dependence of the magnetoresistance $R(T)\equiv[\rho(H=0,T)-\rho(H=H_S,T)]/\rho(H=0,T)$. The squares are the experimental data on [Fe(16 Å)/Cr(12 Å)]$_{18}$ taken from Ref. 1, and the solid line is our fit.

the [Fe(16 Å)/Cr(11 Å)]$_{30}$ sample with small magnetoresistance. By using $S=2$, which is appropriate for iron, we find $\omega_0=435$ K. In Figs. 1–3 the solid lines represent our results, and the solid squares in Figs. 2 and 3 are the experimental data given in Ref. 1. The squares in Fig. 1 represent the *temperature-dependent* resistivity in the sample with large magnetoresistance and putatively rough interfaces that is *above* that coming from the sample with small magnetoresistance (read sharp interfaces) i.e., $\Delta\rho(T)\equiv\rho_a(H,T)-\rho_a(H>H_S,0)-\delta\rho_b(T)$, where a is the sample with large magnetoresistance, and $\delta\rho_b(T)$ is the temperature-dependent part of the resistivity for sample b (small magnetoresistance). In our model we have attributed $\Delta\rho(T)$ to scattering from local magnon modes that exist at *rough* interfaces.

By comparing our calculated temperature-dependent resistivity to the data[1] on [Fe(16 Å)/Cr(12 Å)]$_{18}$, we find that the agreement is excellent. We conclude that it is plausible to model the large *increase* in the temperature-dependent scattering observed in sample with putatively rough interfaces (large magnetoresistance) as arising from thermally activated localized spin flips (magnons). The excitation energy of these modes $\omega_0=435$ K is reasonable. The Curie temperature of iron is $T_C=1043$ K; if we assume that there are one-half as many iron neighbors to an iron atom at a rough Fe/Cr interface, $\omega_0=435$ K is tenable.

In summary, we have modeled the large increase in the temperature dependence of the resistivity of Fe/Cr superlattices with large magnetoresistance, as arising from localized magnon modes at the rough Fe/Cr interfaces. With one new parameter this model is able to reproduce the *enhanced* temperature dependence of the magnetoresistance that has been observed. We have also considered localized phonon modes and find we are unable to fit the enhanced temperature-dependent magnetoresistance in Fig. 3.

We have not discussed the *weak* temperature dependence of the resistivity and magnetoresistance found in samples with small magnetoresistance. Presumably, this comes from magnon and phonon modes that extend over entire Fe or Cr layers or the entire Fe/Cr superlattice in the case of phonons.

ACKNOWLEDGMENTS

We would like to thank Professor A. Fert for informative discussions. This work was supported in part by New York University.

APPENDIX A

The dc conductivity can be calculated by using the standard Kubo formalism[11]

$$\sigma_{xx}=-\lim_{\omega\to 0}\frac{\mathrm{Im}[\Pi_{\mathrm{ret}}(i\omega)]_{xx}}{\omega}\bigg|_{i\omega=\omega+i\delta}, \tag{A1}$$

where

$$[\Pi_{\mathrm{ret}}(i\omega)]_{xx}=\frac{e^2}{m^2}\sum_{\mathbf{k},\sigma}\frac{1}{\beta}\sum_{ip}G^{\sigma}_{\mathbf{k}}(ip)k_x\Gamma^{\sigma}_x(\mathbf{k},ip,ip+i\omega)G^{\sigma}_{\mathbf{k}}(ip+i\omega), \tag{A2}$$

where Γ^{σ} is the vertex function which satisfies the integral equation

$$\Gamma^{\sigma}(\mathbf{k},ip,ip+i\omega)=\mathbf{k}+\sum_{\sigma'}\int\frac{d\mathbf{k}'}{(2\pi)^3}\frac{1}{\beta}\sum_{iq}M^2_{\sigma\sigma'}(\mathbf{k},\mathbf{k}')F^{\sigma'}(\mathbf{k},\mathbf{k}',iq)\times G_{\mathbf{k}',\sigma'}(ip+iq)G_{\mathbf{k}'\sigma'}(ip+iq+i\omega)\Gamma^{\sigma'}(\mathbf{k}',ip+iq,ip+iq+i\omega), \tag{A3}$$

where $G_{\mathbf{k}\sigma}(ip)=1/[ip-\varepsilon_{\mathbf{k}}-\Sigma_{\mathbf{k}\sigma}(ip)]$, $M_{\sigma\sigma'}$ is the matrix element of the interaction between conduction electrons and scattering sources, and F^{σ} is the propagator for the scattering. For example, F^{σ} is a magnon propagator for electron-magnon scattering, and $F^{\sigma}=1$ for electron-impurity scattering with no internal degrees of freedom for the impurities. As pointed out in Sec. II, the corrections to the vertex Γ vanish in some cases, e.g., if the

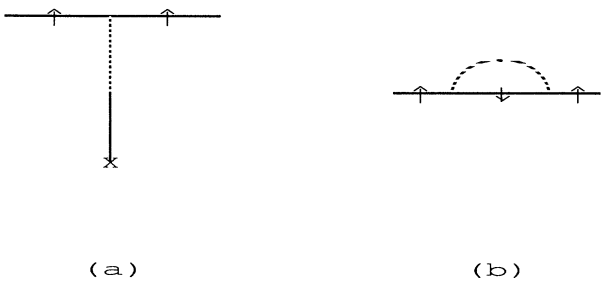

FIG. 4. Self-energies of conduction electrons due to (a) impurity scattering and (b) one-magnon scattering.

scattering takes place in one angular momentum channel and does not conserve momentum $\mathbf{k}$.

Before tackling the integral Eq. (A3), we express the dc conductivity in terms of Γ by summing over frequency ip in Eq. (A2), yielding[11]

$$\sigma=\frac{n_0e^2}{2m}\sum_{\sigma}\int_{-\infty}^{\infty}d\varepsilon\left[-\frac{d}{d\varepsilon}n_F(\varepsilon)\right]\frac{\Lambda^{\sigma}(\varepsilon)}{2\Delta^{\sigma}(\varepsilon)}\ , \tag{A4}$$

where Δ^{σ} is the imaginary part of the conduction-electron self-energy $\Delta^{\sigma}=-\mathrm{Im}\,\Sigma_{\mathbf{k},\sigma}(ip=\varepsilon_F+i\delta)$, and $\Lambda^{\sigma}\equiv\Gamma^{\sigma}\mathbf{k}/|\mathbf{k}|^2$ is the magnitude of the vertex function. For temperatures much lower than the Fermi energy, $-dn_F(\varepsilon)/d\varepsilon$ may be replaced by $\delta(\varepsilon-\varepsilon_F)$ and Eq. (A4) reduces to

$$\sigma=\frac{n_0e^2}{4m}\sum_{\sigma}\frac{\Lambda^{\sigma}(\varepsilon_F)}{\Delta^{\sigma}(\varepsilon_F)}\ . \tag{A5}$$

We now consider the following two cases.

(1) By neglecting vertex corrections, i.e., $\Lambda^{\sigma}=1$, the conductivity is determined by the imaginary parts of the self-energy. The diagrams for the self-energies for impurity and magnon scattering are represented by the diagrams shown in Fig. 4. For impurity scattering, the lowest-order contribution to the self-energy is $V_{\mathrm{imp}}(k=0)$, which is real, so that to first order in V_{imp} it does not contribute to the conductivity Eq. (A5). For magnon scattering as shown in Fig. 4(b), the lowest-order self-energy is V_{mag}^2. We conclude that the lowest order of the scattering potential V to enter the calculation of the conductivity without vertex corrections is V^2. This is the reason that we express our lowest-order t matrix [Eq. (20)] in terms of V^2. It should be pointed out that neglecting vertex corrections does not exclude the spin-flip contribution to the conductivity.

(2) When vertex corrections are important, we must solve the integral equation (A3); generally, this is difficult. However, if we assume that both Δ^{σ} and Λ^{σ} are independent of energy, we may introduce non-spin-flip and spin-flip vertex corrections as shown in Fig. 5. The conductivity from a non-spin-flip (NSF) process Fig. 5(a) is defined as

$$\sigma^{\mathrm{NSF}}(\sigma)\equiv\frac{n_0e^2}{4m}\frac{1}{\tilde{\Delta}(\sigma)}\ , \tag{A6}$$

where $1/\tilde{\Delta}\equiv\Lambda^{\mathrm{NSF}}/\Delta$, while that from a spin-flip (SF) process Fig. 5(b) is defined as

$$\sigma^{\mathrm{SF}}(\sigma)=\frac{n_0e^2}{4m}\frac{1}{\tilde{\Delta}(\sigma)}\frac{P}{\tilde{\Delta}(-\sigma)}\ , \tag{A7}$$

where P denotes the spin-flip scattering matrix. The conductivity is obtained by summing the ladder diagrams shown in Fig. 5(c), which consist of repeated use of the basic vertices [Figs. 5(a) and 5(b)], and we find

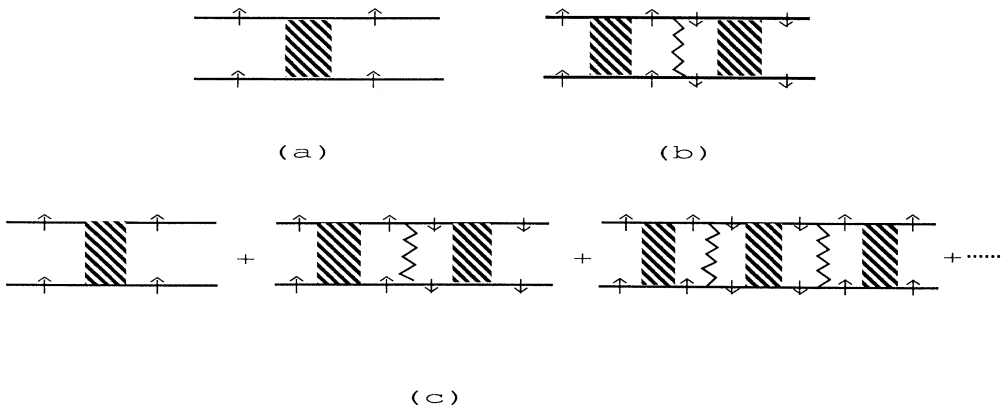

FIG. 5. Contributions to the conductivity from (a) a non-spin-flip ladder diagram, (b) a spin-flip ladder diagram (the zigzag line), and (c) all possible ladder diagrams for non-spin-flip and spin-flip processes.

$$\sigma(\sigma)=\frac{n_0e^2}{4m}\frac{1}{\tilde{\Delta}(\sigma)}\left[1+\frac{P}{\tilde{\Delta}(-\sigma)}\right]\times\left[1+\frac{P^2}{\tilde{\Delta}(\sigma)\tilde{\Delta}(-\sigma)}+\cdots\right]=\frac{n_0e^2}{4m}\frac{\tilde{\Delta}(-\sigma)+P}{\tilde{\Delta}(\sigma)\tilde{\Delta}(-\sigma)-P^2}\ . \tag{A8}$$

By defining the resistivity ρ_σ and "spin-mixing" $\rho_{\uparrow\downarrow}$ as

$$\rho_\sigma=\left[\frac{n_0e^2}{4m}\frac{1}{\tilde{\Delta}(\sigma)-P}\right]^{-1} \tag{A9}$$

and

$$\rho_{\uparrow\downarrow}=\left[\frac{n_0e^2}{4m}P\right]^{-1},$$

we find

$$\sigma=\sum_\sigma\sigma(\sigma)=\frac{\rho_\uparrow+\rho_\downarrow+4\rho_{\uparrow\downarrow}}{\rho_\uparrow\rho_\downarrow+\rho_{\uparrow\downarrow}(\rho_\uparrow+\rho_\downarrow)}\ . \tag{A10}$$

This is exactly the two-current model derived by Fert by using the Boltzmann equation. By comparing the two expressions ρ_σ and $\rho^{\mathrm{NSF}}=(\sigma^{\mathrm{NSF}})^{-1}$, we note that they are different: ρ^{NSF} contains only vertices of type Fig. 5(a), while ρ_σ contains both types of vertices, Figs. 5(a) *and* 5(b), and has the final spin direction, after all successive scattering events, the same as the initial, i.e., no spin mixing.

APPENDIX B

The conventional approach to calculating the conduction-electron lifetime due to spin-flip processes follows the method developed by Van Peski-Tinbergen and Dekker.[12] The relaxation time can be cast into the form[12]

$$\frac{1}{\tau}(k,\sigma)=\sum_{mm'\sigma'}\omega_m e^{-\beta E_m}\left\{\frac{1}{1-f(\varepsilon_{\mathbf{k}})[1-e^{-\beta(E_{m'}-E_m)}]}\right\}\times\int\frac{d\mathbf{k}'}{(2\pi)^3}|\langle k'\sigma'm'|V(\sigma)|k\sigma m\rangle|^2\times\delta(\varepsilon_{k'}-\varepsilon_k+E_{m'}-E_m)\ , \tag{B1}$$

where $V(\sigma)$ is the scattering potential [Eq. (6)], E_m is the energy of the local state, $f(\varepsilon)$ is the Fermi function, and the expression in curly brackets accounts for the inelasticity in the collisions. By evaluating the matrix elements of the scattering potential Eq. (6) and limiting ourselves to the spin-flip terms, we find the conventional result[12]

$$\frac{1}{\tau_\pm(k)}\sim\frac{\rho(\varepsilon_k\pm\omega)[S(S+1)\mp\langle S_z\rangle-\langle S_z^2\rangle]}{1-f(\varepsilon_k)(1-e^{\mp\beta\omega})}\ , \tag{B2}$$

where $\omega\equiv E_{m-1}-E_m$, and the angular brackets denote a thermal average over the energy of the local state.

While this expression for the spin flip looks quite different from Eq. (17), interalia, the spin dependence ($\pm$) in Eq. (B2), while Eq. (18) states they are independent of spin in the spin-wave approximation (SWA), the two are identical. To establish this set $f(\varepsilon_k)=\frac{1}{2}$; while this is not done in the conventional treatments of the magnetoresistance, it is permissible in our calculation, because in our case it appears in the denominator of the expressions over which we eventually integrate with the factor $\partial f(\varepsilon)/\partial\varepsilon$, whereas in the magnetoresistance calculation it appears in the numerator. In the SWA,

$$\langle S^+S^-\rangle=S(S+1)+\langle S_z\rangle-\langle S_z^2\rangle\approx 2S[1+n^B(\omega)] \tag{B3a}$$

and

$$\langle S^-S^+\rangle=S(S+1)-\langle S_z\rangle-\langle S_z^2\rangle\approx 2Sn^B(\omega)\ . \tag{B3b}$$

By placing Eqs. (B3) in (B2) and setting $f(\varepsilon)=\frac{1}{2}$, we find

$$\frac{1}{\tau_\pm}\sim\frac{4S\rho(\varepsilon_F\pm\omega)}{(1+e^{-\beta\omega})(e^{\beta\omega}-1)}=2S\rho(\varepsilon_F\pm\omega)[n^B(\omega)+n^F(\omega)]\ . \tag{B4}$$

Thus we see that seemingly different relaxation rates due to spin-flip scattering are in fact the same in the SWA, if we make the reasonable assumption that the conduction-electron density of states is rather flat near the Fermi surface, i.e., $\rho(\varepsilon_F\pm\omega)\approx\rho(\varepsilon_F)$ for $\omega\ll\varepsilon_F$.

---

*Present address: Physics Department B-019, University of California, San Diego, La Jolla, CA 92093.

[1]F. Petroff, A. Barthélémy, A. Hamzic, A. Fert, P. Etienne, S. Lequien, and G. Creuzet, J. Magn. Magn. Mater (to be published).

[2]P. M. Levy, S. Zhang, and A. Fert, Phys. Rev. Lett. **65**, 1643 (1990); (unpublished).

[3]A. Fert and I. A. Campbell, J. Phys. F **6**, 849 (1976).

[4]A. Fert, J. Phys. C **2**, 1784 (1969).

[5]Electron-electron scattering contributes to both $\rho_{i\sigma}(T)$ and $\rho_{\uparrow\downarrow}(T)$. However, except for very low temperatures, its contribution is small compared with those coming from phonons and magnons. See A. Bourquard, E. Daniel, and A. Fert, Phys. Lett. **26A**, 260 (1968).

[6]B. Loegel and F. Gautier, J. Phys. Chem. Solids **32**, 2723 (1971).

[7]D. L. Mills, A. Fert, and I. A. Campbell, Phys. Rev. B **4**, 196 (1971).

[8]This condition is the reason there are no vertex corrections to the resistivity of the impurity Anderson model in which resonant scattering occurs in *one* angular momentum channel. See Appendix D of N. E. Bickers, D. L. Cox, and J. W. Wilkins, Phys. Rev. B **36**, 2036 (1987).

[9]Y. Wang, P. M. Levy, and J. L. Fry, Phys. Rev. Lett. **65**, 2732

(1990).
[10]Localized magnons are discussed by M. F. Thorpe, in *Correlation Functions and Quasiparticle Interactions in Condensed Matter*, edited by J. Woods Halley (Plenum, New York, 1978), p. 274.
[11]G. D. Mahan, *Many-Particle Physics* (Plenum, New York, 1981), Chap. 3, Sec. 5 and Chap. 7, Sec. 3.
[12]T. Van Peski-Tinbergen and A. J. Dekker, Physica (Utrecht) **29**, 917 (1963); M. T. Béal-Monod and R. A. Weiner, Phys. Rev. **170**, 552 (1968); W. Guo and P. M. Levy, Phys. Rev. B **37**, 6676 (1988).